Available online at www.sciencedirect.com
SCIENCE DIRECT
Journal of Sound and Vibration 295 (2006) 461–478
JOURNAL OF SOUND AND VIBRATION
www.elsevier.com/locate/jsvi

Longitudinal wave propagation. Part I—Comparison of rod theories

Marek Krawczuk[a,b,*], Joanna Grabowska[a], Magdalena Palacz[a]

[a]Institute of Fluid Flow Machinery PAS, Fiszera 14, 80–952 Gdańsk, Poland
[b]Department of Electrical Engineering and Automatic, Technical University of Gdańsk, Narutowicza 11/12, 80–952 Gdańsk, Poland

Received 5 January 2004; received in revised form 14 November 2005; accepted 19 December 2005
Available online 23 March 2006

Abstract

The paper introduces new four spectral elements for analysis of longitudinal wave propagation in structures. The developed elements are based on the elementary, Love, Mindlin–Herrmann and three-mode theories. Certain differences in wave propagation behaviour are observed for the analysed models. For lower excitation frequencies the results obtained for all models are similar and from a practical point of view the spectral element based on the Love theory is adequate. For high frequency excitation these differences are considerable and only the Mindlin–Herrmann or three-mode models give correct results.

1. Introduction

Wave propagation in structural elements has been studied over a considerable period of time. Although mathematical frameworks are well developed, wave propagation problems in real scale engineering structures are an open area of research. The main problems in analysis of propagation of high velocity waves in distributed structures are that spatial discretisation must be accurate to capture the amplified effect of wave scattering at structural discontinuities. A conventional modal method, when extended to the high frequency regime, becomes computationally inefficient since many higher modes that participate in motion will not be represented. For a specific geometry and finite, periodic or semi-infinite boundary conditions, many solution techniques have been reported [1–3]. Among many frequency domain methods, the spectral element method [4] has been found suitable for analysis of wave's propagation in real engineering structures.

The spectral element method utilises the exact solution of differential equations governing the problem. This exact solution is used as an interpolating function for the spectral element formulation. The use of the exact solution in the element formulation ensures the exact mass and stiffness distribution. It means that only one element can be used for modelling a very large part of a structure, under the condition that this part has no

*Corresponding author. Institute of Fluid Flow Machinery, Polish Academy of Sciences, Fiszera 14, 80–952 Gdańsk, Poland. Tel.: +48 58 341 12 71X206; fax: +48 58 341 44 61.
E-mail address: mk@imp.gda.pl (M. Krawczuk).

0022-460X/$ - see front matter
doi:10.1016/j.jsv.2005.12.048

discontinuities. Hence, the problem size is much smaller in comparison to the conventional finite element formulation.

For example, in order to properly model wave propagation at frequency about 200 kHz, in a cantilever rod with length of 6 m and cross section 0.02×0.02 m almost 465 rod finite elements are needed. It means that the length of one element is about 0.012 m, and it seems that they are not rods in a physical sense. Obviously it is possible to use other types of finite elements (e.g. 3D-solids), but in this case the size of problem is even greater. It means that numerical calculation time is long and errors of numerical integration can be considerable. The spectral analysis allows use of one spectral element for any length provided there are no changes in the cross section or material parameters. If that happens it is very simple to join several spectral elements in a way that is commonly used in finite element methods.

The spectral element program architecture is very similar to the architecture of a typical finite element program as far as the assembly and the solution is considered. Firstly, the excitation function is split up into a number of frequency components using the forward Fourier transform. Next, as a part of a big frequency do-loop (as opposed to a do-loop over time step in the conventional finite element formulation), the dynamic stiffness matrix is generated, transformed and solved for every frequency. This directly yields to the frequency response function of the analysed problem. The frequency domain responses are then transformed to the time domain using the inverse Fourier transform.

The spectral elements are available for rods [5–6], beams [7–8], plates [9–11], and layered solids [12]. For rod elements one can find spectral elements developed on the basis of elementary rod theory; however, there are no spectral elements which are based on modified theories. Such elements would be suitable for analysis of waves propagating at higher frequencies. Apart from that they take into account more realistic assumptions concerning longitudinal and transverse deformations. Problems of longitudinal wave propagation have been analysed up till now using the elementary theory, under assumption of a constant longitudinal displacement along the cross section of the rod and also neglecting transverse deflection [5–6]. The real deformation of the rod is more complicated, and in broad terms three characteristic types of behaviour can be identified. The first is that the longitudinal displacement has a non-zero mean value (Love rod theory), the second is that the transverse deflection is nearly linear (Mindlin–Herrmann rod theory), and the third is that the longitudinal displacement has almost a parabolic distribution (three-mode rod theory). It means that higher order theories should have two additional deformation modes—the transverse deflection and the parabolic longitudinal displacement along the rod.

In the presented paper new spectral elements for analysis of longitudinal waves in rods are developed. The elements are based on the Love [13], Mindlin–Herrmann [14], and three-mode theories [15]. In the case of the Love theory, the spectral element has two nodes with one longitudinal degree of freedom at each node. For the Mindlin–Herrmann theory the spectral element has two nodes and two degrees of freedom at each node—the longitudinal displacement, and a rotation which describes transverse contraction. In case of the three-mode theory the element has two nodes and three degrees of freedom at each node. These are the longitudinal displacement, the rotation which describes the transverse contraction and second rotation, which models the parabolic distribution of the axial displacement along the height of the element.

A procedure for building the explicit form of the dynamic stiffness matrix for all the models is precisely explained. Numerical examples presented illustrate the wave propagation process in rods for every model, respectively. Considerable differences in the behaviour of longitudinal waves in rods for the modified theories are shown what is widely described in the paper.

2. Elementary theory

A spectral element model of rod based on the elementary theory is shown in Fig. 1a. The element has length L and constant cross section A. There are two nodes with one longitudinal degree of freedom per node.

The elementary theory assumes that the axial deformations along the neutral axis of the rod are the same in all points of the cross section, and also the transverse deflections are negligible. The differential equation of the

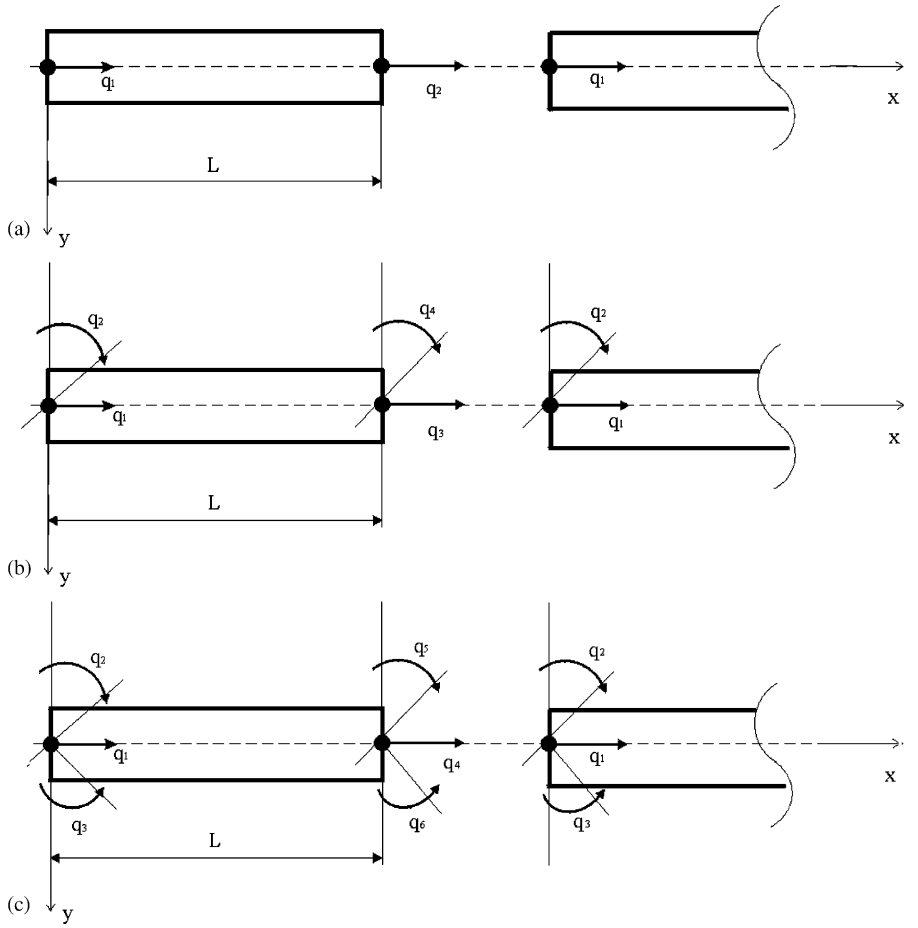

Fig. 1. The spectral element models for the elementary and Love theories (a), the Mindlin–Herrmann theory (b) and the three-mode theory (c).

problem can be written as follows:

$$EA\frac{\partial^2 u_0}{\partial x^2} - \rho A\frac{\partial^2 u_0}{\partial t^2} = 0, \tag{1}$$

with the boundary condition on u_0 as

$$u_0, \quad Q_u = EA\frac{\partial u_0}{\partial x}, \tag{2}$$

where u_0 is the average axial displacement, Q_u means the longitudinal force, E denotes the Young's modulus, A is the area of the cross section of the rod and ρ is the density of the material.

The spectral element for this theory was established by Doyle [5]. The dynamic stiffness matrices for the two node spectral element $\mathbf{K}_{\mathrm{df}}$ and the throw-off element $\mathbf{K}_{\mathrm{dt}}$ can be presented in the following forms:

$$\mathbf{K}_{\mathrm{df}} = \frac{\mathrm{i}kEA}{(1-\mathrm{e}^{-2\mathrm{i}kL})}\begin{bmatrix} 1+\mathrm{e}^{-2\mathrm{i}kL} & -2\mathrm{e}^{-\mathrm{i}kL} \\ -2\mathrm{e}^{-\mathrm{i}kL} & 1+\mathrm{e}^{-2\mathrm{i}kL} \end{bmatrix}, \quad \mathbf{K}_{\mathrm{dt}} = \mathrm{i}kEA, \tag{3}$$

where k is the wavenumber calculated as a function of the frequency ω and material properties ρ, E:

$$k = \pm\omega\sqrt{\frac{\rho}{E}}. \tag{4}$$

3. Love theory

A spectral element model of rod based on the Love theory is also presented in Fig. 1a. The element has the same length and the constant cross section as the one calculated with the elementary theory. The aforementioned element has two nodes with one longitudinal degree of freedom per node. The Love theory modification is based on the assumption that each material point of the rod has a transverse velocity. It means that the kinetic energy is affected by additional terms; however, the strain energy is the same as for the elementary rod theory. The displacement field is also the same, and the differential equation of the problem is only slightly modified. This can be expressed in the following form [13]:

$$EA\frac{\partial^2 u_0}{\partial x^2}+\nu^2\rho J\frac{\partial^2}{\partial x^2}\left(\frac{\partial^2 u_0}{\partial t^2}\right)-\rho A\frac{\partial^2 u_0}{\partial t^2}=0, \tag{5}$$

with the boundary condition on u_0 as

$$u_0, \quad Q_u=EA\frac{\partial u_0}{\partial x}+\nu^2\rho J\frac{\partial^2 u_0}{\partial t^2}. \tag{6}$$

The term J denotes the polar moment of inertia of the rod cross section, and ν is the Poisson ratio of the material.

The wavenumber for this model is given by the relation:

$$k=\pm\omega\sqrt{\frac{\rho A}{EA-\nu^2\rho J\omega^2}}. \tag{7}$$

It should be noticed that the wavenumber k, in contrast to the elementary theory, can be purely imaginary. In such case the transverse motion is absorbing all the input energy.

3.1. Rod spectral element for Love theory

The general longitudinal displacement of a rod can be written in the same form as for the elementary theory:

$$\hat{u}_0=A_0\mathrm{e}^{-\mathrm{i}kx}+B_0\mathrm{e}^{-\mathrm{i}k(L-x)}. \tag{8}$$

Constants A_0 and B_0 can be found from the following nodal conditions:

$$\hat{u}_0(x=0)=\hat{q}_1, \quad \hat{u}_0(x=L)=\hat{q}_2, \tag{9}$$

which lead to the following system of equations:

$$\begin{bmatrix}A_0\\B_0\end{bmatrix}=\begin{bmatrix}1 & p\\ p & 1\end{bmatrix}^{-1}\begin{bmatrix}\hat{q}_1\\ \hat{q}_2\end{bmatrix}, \tag{10}$$

with $p=\mathrm{e}^{-\mathrm{i}kL}$.

The forces within the element can be expressed using formulas from Eq. (6) by differentiating the assumed displacements. The nodal forces can be found using the following nodal conditions:

$$\begin{aligned}\hat{F}_1&=EA\frac{\partial\hat{u}_0}{\partial x}+\nu^2\rho J\frac{\partial^2\hat{u}_0}{\partial t^2} \quad \text{for } x=0,\\ \hat{F}_2&=EA\frac{\partial\hat{u}_0}{\partial x}+\nu^2\rho J\frac{\partial^2\hat{u}_0}{\partial t^2} \quad \text{for } x=L.\end{aligned} \tag{11}$$

Taking into account formulas for the axial displacement the nodal forces are given by the following expression:

$$\begin{bmatrix}\hat{F}_1\\ \hat{F}_2\end{bmatrix}=\begin{bmatrix}\mathrm{i}k\left(-EA+\rho\nu^2J\omega^2\right) & \mathrm{i}k\left(-EA+\rho\nu^2J\omega^2\right)p\\ \mathrm{i}k\left(-EA+\rho\nu^2J\omega^2\right)p & \mathrm{i}k\left(-EA+\rho\nu^2J\omega^2\right)\end{bmatrix}\begin{bmatrix}A_0\\B_0\end{bmatrix}. \tag{12}$$

Then using the formulas for calculating constants A_0 and B_0 as a function of the nodal displacements, the relation between the nodal forces and the nodal displacements can be calculated. The square and symmetric matrix in this relation denotes the dynamic stiffness matrix $\mathbf{K}_{df}$ of the spectral element based on the Love theory.

3.2. Throw-off spectral element for Love theory

For the throw-off element based of the Love theory the general longitudinal displacement for a rod can be written is the same form as for the elementary theory:

$$\hat{u}_0 = A_0 e^{-ikx}. \tag{13}$$

The constant A_0 can be found from the following nodal condition:

$$\hat{u}_0(x=0) = \hat{q}_1, \tag{14}$$

which leads to the equation:

$$A_0 = \hat{q}_1. \tag{15}$$

The forces within the element can be expressed using the formulas from Eq. (6). The nodal forces can be found using the following nodal condition:

$$\hat{F}_1 = EA\frac{\partial \hat{u}_0}{\partial x} + v^2\rho J\frac{\partial^2 \hat{u}_0}{\partial t^2} \quad \text{for } x = 0. \tag{16}$$

Taking into account the formulas for the axial displacements and the lateral contractions the nodal forces are given by the expression:

$$\hat{F}_1 = ik(-EA + \rho v^2 J\omega^2)\hat{q}_1. \tag{17}$$

The relation in the brackets in Eq. (17) denotes the dynamic stiffness matrix $\mathbf{K}_{dt}$ of the throw-off spectral element based on the Love theory.

4. Mindlin–Herrmann theory (two-mode)

A spectral element model of rod based on the Mindlin–Herrmann theory is presented in Fig. 1b. The element has the same geometry as in two previously described cases. It has also two nodes with two degrees of freedom per node (the longitudinal displacement and the rotation). The Mindlin–Herrmann theory can be developed taking into account independent shearing deformation due to transverse displacement. The displacements in Mindlin–Herrmann theory of rods are assumed as follows [4]:

$$\begin{aligned} u(x,y) &= u_0(x), \\ v(x,y) &= \psi_0(x)\cdot y, \end{aligned} \tag{18}$$

where ψ_0 denotes the transverse contraction.

This approach takes into account the lateral displacements but ignores the non-uniform distribution of the axial displacement in the cross section of the rod. The differential equations for the Mindlin–Herrmann theory, governing the rod vibration problem are [4]:

$$\begin{aligned} &(2\mu+\lambda)A\frac{\partial^2 u_0}{\partial x^2} + \lambda A\frac{\partial \psi_0}{\partial x} = \rho A\frac{\partial^2 u_0}{\partial t^2} - q, \\ &\mu I K_1\frac{\partial^2 \psi_0}{\partial x^2} - (2\mu+\lambda)A\psi - \lambda A\frac{\partial u_0}{\partial x} = \rho I K_2\frac{\partial^2 \psi_0}{\partial t^2} \end{aligned} \tag{19}$$

with the associated boundary conditions (at each end of the rod):

$$u_0, \quad Q_u = (2\mu+\lambda)A\frac{\partial u_0}{\partial x} + \lambda A\psi_0,$$
$$\psi_0, \quad Q_\psi = \mu I K_1\left(\frac{\partial \psi_0}{\partial x}\right), \tag{20}$$

where $\mu = E/(2(1+\nu)), \lambda = \nu E/((1+\nu)(1-2\nu))$ and I is the geometrical moment of the rod cross section.

Parameters K_1 and K_2 are calculated from the formulas:

$$K_1 = \frac{12}{\pi^2}, \quad K_2 = K_1\left(\frac{1+\nu}{0.87+1.12\nu}\right)^2. \tag{21}$$

These parameters are a set of coupled equations for the longitudinal displacement and lateral contraction. Since there are two dependent variables u_0 and ψ_0, and the coefficients are constant, to obtain the spectrum relation one assumes solutions in the forms:

$$u_0 = U\mathrm{e}^{-\mathrm{i}(kx-\omega t)}, \quad \psi_0 = \Psi\mathrm{e}^{-\mathrm{i}(kx-\omega t)}. \tag{22}$$

After the substitution into differential equations the following system is obtained:

$$\begin{bmatrix} -(2\mu+\lambda)Ak^2+\rho A\omega^2 & -\mathrm{i}k\lambda A \\ \mathrm{i}k\lambda A & -\mu I K_1 k^2 - (2\mu+\lambda)A + \rho I K_2\omega^2 \end{bmatrix}\begin{bmatrix} U \\ \Psi \end{bmatrix} = \begin{bmatrix} 0 \\ 0 \end{bmatrix}. \tag{23}$$

Setting the determinant equal to zero gives the characteristic equation for determining k as

$$a_2k^4 + a_1k^2 + a_0 = 0, \tag{24}$$

where

$$\begin{aligned} a_2 &= \mu A I K_1(2\mu+\lambda), \\ a_1 &= \left[4\mu(\mu+\lambda)A^2 - \rho I K_2\omega^2(2\mu+\lambda)A - \rho A\omega^2\mu I K_1\right], \\ a_0 &= -\rho A\omega^2\left[A(2\mu+\lambda) - \rho I K_2\omega^2\right]. \end{aligned} \tag{25}$$

This characteristic equation is quadratic in k^2 and therefore, there are two-mode pairs in contrast to the single pair of the elementary and Love theories.

4.1. Rod spectral element for the Mindlin–Herrmann theory

The general longitudinal displacement and rotation of a rod can be written as

$$\begin{aligned} \hat{u}_0 &= A_0R_1\mathrm{e}^{-\mathrm{i}k_1x} + B_0R_2\mathrm{e}^{-\mathrm{i}k_2x} - C_0R_1\mathrm{e}^{-\mathrm{i}k_1(L-x)} - D_0R_2\mathrm{e}^{-\mathrm{i}k_2(L-x)}, \\ \hat{\psi}_0 &= A_0\mathrm{e}^{-\mathrm{i}k_1x} + B_0\mathrm{e}^{-\mathrm{i}k_2x} + C_0\mathrm{e}^{-\mathrm{i}k_1(L-x)} + D_0\mathrm{e}^{-\mathrm{i}k_2(L-x)}, \end{aligned} \tag{26}$$

where R_i are the amplitude ratios given by

$$R_i = \frac{\mathrm{i}k_i\lambda A}{-(2\mu+\lambda)Ak_i^2 + \rho A\omega^2}, \quad i = 1,2. \tag{27}$$

Constants A_0, B_0, C_0 and D_0 can be found from the following nodal conditions:

$$\begin{aligned} &\hat{u}_0(x=0) = \hat{q}_1, \quad \hat{\psi}_0(x=0) = \hat{q}_2, \\ &\hat{u}_0(x=L) = \hat{q}_3, \quad \hat{\psi}_0(x=L) = \hat{q}_4. \end{aligned} \tag{28}$$

The forces within the element can be expressed by differentiating the formulas from Eq. (26) and by using the following nodal conditions:

$$\hat{F}_1 = (2\mu+\lambda)A\frac{\partial \hat{u}_0}{\partial x} + \lambda A\psi_0 \quad \text{for } x=0, \quad \hat{F}_2 = \mu I K_1\left(\frac{\partial \hat{\psi}_0}{\partial x}\right) \quad \text{for } x=0,$$
$$\hat{F}_3 = (2\mu+\lambda)A\frac{\partial \hat{u}_0}{\partial x} + \lambda A\psi_0 \quad \text{for } x=L, \quad \hat{F}_4 = \mu I K_1\left(\frac{\partial \hat{\psi}_0}{\partial x}\right) \quad \text{for } x=L, \tag{29}$$

Taking into account the formulas for the axial displacement and rotation with the formulas for calculating constants A_0, B_0, C_0 and D_0 it is possible to express the nodal forces as a function of nodal displacements. The relation between the nodal displacements and the nodal forces contains the square and symmetric matrix which is the dynamic stiffness matrix $\mathbf{K}_{\mathrm{df}}$ of the rod spectral element based on the Mindlin–Herrmann theory (see Appendix A for the exact mathematical form).

4.2. Throw-off spectral element for the Mindlin–Herrmann theory

For the throw-off element based on the Mindlin–Herrmann theory the axial displacement and the rotation are given by:

$$\hat{u}_0 = A_0 R_1 \mathrm{e}^{-\mathrm{i}k_1 x} + B_0 R_2 \mathrm{e}^{-\mathrm{i}k_2 x},$$
$$\hat{\psi}_0 = A_0 \mathrm{e}^{-\mathrm{i}k_1 x} + B_0 \mathrm{e}^{-\mathrm{i}k_2 x}. \tag{30}$$

The constants A_0 and B_0 can be found from the following nodal conditions:

$$\hat{u}_0(x=0) = \hat{q}_1, \quad \hat{\psi}_0(x=0) = \hat{q}_2. \tag{31}$$

The forces within the element can be expressed by manipulating Eqs. (26)–(28) as before. The nodal forces can be found using the following nodal conditions:

$$\hat{F}_1 = (2\mu+\lambda)A\frac{\partial \hat{u}_0}{\partial x} + \lambda A\psi_0 \quad \text{for } x=0, \quad \hat{F}_2 = \mu I K_1\left(\frac{\partial \hat{\psi}_0}{\partial x}\right) \quad \text{for } x=0. \tag{32}$$

The square and symmetric dynamic stiffness matrix for the throw-off element based on the Mindlin–Herrmann theory is calculated with the same algorithm as for the elements described previously. Specified formulae can be found in Appendix A, Eq. (A.4).

5. Three-mode theory

A spectral element model of rod based on the three-mode theory, with the same geometry as three previously described elements, is presented in Fig. 1c. The element has two nodes with three degrees of freedom per node (the longitudinal displacement and two rotations). The displacements in the three-mode theory of a rod are assumed as follows [4]:

$$u(x,y) = u_0(x) + \phi_0(x)\cdot h\left(1 - 12\frac{y^2}{h^2}\right),$$
$$v(x,y) = \psi_0(x)\cdot y, \tag{33}$$

where ϕ_0 is a function which describes a parabolic distribution of the axial displacement along the height of the rod, and h denotes the height of the rod.

The differential equations for the three-mode theory, governing the rod vibration problem are given by [4]

$$(2\mu+\lambda)A\frac{\partial^2 u_0}{\partial x^2} + \lambda A\frac{\partial \psi_0}{\partial x} = \rho A\frac{\partial^2 u_0}{\partial t^2} - q,$$
$$\mu I\frac{\partial^2 \psi_0}{\partial x^2} - (2\mu+\lambda)A\psi - \lambda A\frac{\partial u_0}{\partial x} - 2\mu A h\frac{\partial \phi_0}{\partial x} = \rho I\frac{\partial^2 \psi_0}{\partial t^2},$$
$$(2\mu+\lambda)I\frac{\partial^2 \phi_0}{\partial x^2} - 5\mu A\phi + \frac{10}{48}\mu A h\frac{\partial \psi_0}{\partial x} = \rho I\frac{\partial^2 \phi_0}{\partial t^2}, \tag{34}$$

with the associated boundary conditions (at each end of the rod):

$$u_0, \quad Q_u = (2\mu+\lambda)A\frac{\partial u_0}{\partial x} + \lambda A\psi_0,$$
$$\psi_0, \quad Q_\psi = \mu I\left(\frac{\partial \psi_0}{\partial x} - 24\frac{\phi_0}{h}\right),$$
$$\phi_0, \quad Q_\phi = \frac{48}{5}(2\mu+\lambda)I\frac{\partial \phi_0}{\partial x}. \tag{35}$$

They are a set of coupled equations for the longitudinal displacement and the lateral contractions. Since there are three dependent variables u_0, ϕ_0 and ψ_0, and the coefficients are constant, to obtain the spectrum relation one has to assume solutions in the forms:

$$u_0 = U\mathrm{e}^{-\mathrm{i}(kx-\omega t)}, \quad \psi_0 = \Psi\mathrm{e}^{-\mathrm{i}(kx-\omega t)}, \quad \phi_0 = \Phi\mathrm{e}^{-\mathrm{i}(kx-\omega t)}. \tag{36}$$

After substituting Eq. (36) into Eq. (34) a system of algebraic equations can be written as

$$\begin{bmatrix} -(2\mu+\lambda)Ak^2+\rho A\omega^2 & -\mathrm{i}k\lambda A & 0 \\ \mathrm{i}k\lambda A & -\mu Ik^2-(2\mu+\lambda)A+\rho I\omega^2 & 2\mathrm{i}k\mu Ah \\ 0 & -\frac{10}{48}\mathrm{i}\mu Ah & -(2\mu+\lambda)Ik^2-5\mu A+\rho I\omega^2 \end{bmatrix}\begin{bmatrix} U \\ \Psi \\ \Phi \end{bmatrix} = \begin{bmatrix} 0 \\ 0 \\ 0 \end{bmatrix}. \tag{37}$$

Setting the determinant equal to zero gives the characteristic equation for determining k as

$$a_3k^6 + a_2k^4 + a_1k^2 + a_0 = 0, \tag{38}$$

where

$$\begin{aligned} a_3 &= -AI^2\mu(2\mu+\lambda)^2, \\ a_2 &= -AI(2\mu+\lambda)\left[4A\mu(\mu+\lambda) - I(4\mu+\lambda)\rho\omega^2\right], \\ a_1 &= A\left[-20A^2\mu^2(\mu+\lambda) + AI\left(\lambda^2+13\lambda\mu+18\mu^2\right)\rho\omega^2 - I^2(5\mu+2\lambda)\rho^2\omega^4\right], \\ a_0 &= \rho A\omega^2\left(5A\mu-\rho I\omega^2\right)\left[A(2\mu+\lambda)-\rho I\omega^2\right]. \end{aligned} \tag{39}$$

This characteristic equation is cubic in k^2 and therefore there are three-mode pairs in contrast to the single pair of the elementary and Love theories, as well as the two-mode pairs of the Mindlin–Herrmann theory.

5.1. Rod spectral element for the three-mode theory

The general longitudinal displacement and rotations of a rod can be written as

$$\begin{aligned} \hat{u}_0 &= A_0R_4\mathrm{e}^{-\mathrm{i}k_1x} + B_0R_5\mathrm{e}^{-\mathrm{i}k_2x} + C_0R_6\mathrm{e}^{-\mathrm{i}k_3x} + D_0R_4\mathrm{e}^{-\mathrm{i}k_1(L-x)} + E_0R_5\mathrm{e}^{-\mathrm{i}k_2(L-x)} + F_0R_6\mathrm{e}^{-\mathrm{i}k_3(L-x)}, \\ \hat{\psi}_0 &= A_0R_1\mathrm{e}^{-\mathrm{i}k_1x} + B_0R_2\mathrm{e}^{-\mathrm{i}k_2x} + C_0R_3\mathrm{e}^{-\mathrm{i}k_3x} - D_0R_1\mathrm{e}^{-\mathrm{i}k_1(L-x)} - E_0R_2\mathrm{e}^{-\mathrm{i}k_2(L-x)} - F_0R_3\mathrm{e}^{-\mathrm{i}k_3(L-x)}, \\ \hat{\phi}_0 &= A_0\mathrm{e}^{-\mathrm{i}k_1x} + B_0\mathrm{e}^{-\mathrm{i}k_2x} + C_0\mathrm{e}^{-\mathrm{i}k_3x} + D_0\mathrm{e}^{-\mathrm{i}k_1(L-x)} + E_0\mathrm{e}^{-\mathrm{i}k_2(L-x)} + F_0\mathrm{e}^{-\mathrm{i}k_3(L-x)}, \end{aligned} \tag{40}$$

where the amplitude ratios are given by

$$\begin{aligned} R_i &= \frac{(2\mu+\lambda)Ik_i^2 + 5\mu A - \rho I\omega^2}{-\frac{10}{48}\mathrm{i}\mu Ah}, \quad i = 1,2,3, \\ R_i &= \frac{\mathrm{i}k_j\lambda A}{-(2\mu+\lambda)Ak_j^2+\rho A\omega^2}R_j, \quad i = 4,5,6, \quad j = 1,2,3. \end{aligned} \tag{41}$$

The constants A_0, B_0, C_0, D_0, E_0 and F_0 can be found from the following nodal conditions:

$$\begin{aligned} &\hat{u}_0(x=0) = \hat{q}_1, \quad \hat{\psi}_0(x=0) = \hat{q}_2, \quad \hat{\phi}_0(x=0) = \hat{q}_3, \\ &\hat{u}_0(x=L) = \hat{q}_4, \quad \hat{\psi}_0(x=L) = \hat{q}_5, \quad \hat{\phi}_0(x=L) = \hat{q}_6, \end{aligned} \tag{42}$$

which lead to the system of equations presented in Appendix B (Eq. (B.4)).

The forces within element can be expressed using the formulas from Eq. (35). The nodal forces can be found using the nodal conditions as follows:

$$\begin{aligned}
\hat{F}_1 &= (2\mu+\lambda)A\frac{\partial\hat{u}_0}{\partial x}+\lambda A\hat{\psi}_0 \quad \text{for } x=0,\\
\hat{F}_2 &= \mu I\left(\frac{\partial\hat{\psi}_0}{\partial x}-24\frac{\hat{\phi}_0}{h}\right) \quad \text{for } x=0,\\
\hat{F}_3 &= \frac{48}{5}(2\mu+\lambda)I\frac{\partial\hat{\phi}_0}{\partial x} \quad \text{for } x=0,\\
\hat{F}_4 &= (2\mu+\lambda)A\frac{\partial\hat{u}_0}{\partial x}+\lambda A\hat{\psi}_0 \quad \text{for } x=L,\\
\hat{F}_5 &= \mu I\left(\frac{\partial\hat{\psi}_0}{\partial x}-24\frac{\hat{\phi}_0}{h}\right) \quad \text{for } x=L,\\
\hat{F}_6 &= \frac{48}{5}(2\mu+\lambda)I\frac{\partial\hat{\phi}_0}{\partial x} \quad \text{for } x=L.
\end{aligned} \tag{43}$$

Taking into account the formulas for the axial displacement and the lateral contractions and using the formulas for calculating constants A_0, B_0, C_0, D_0, E_0 and F_0 as a function of the nodal displacements the relation between the nodal forces and the nodal displacements can be calculated. The square and symmetric matrix in this equation denotes the dynamic stiffness $\mathbf{K}_{\mathrm{df}}$ matrix of the spectral element based on the three-mode theory (Appendix B, Eq. (B.4)).

5.2. Throw-off spectral element for the three-mode theory

For the throw-off spectral element based on the three-mode theory the axial displacement and the lateral contractions are:

$$\begin{aligned}
\hat{u}_0 &= A_0R_4\mathrm{e}^{-\mathrm{i}k_1x}+B_0R_5\mathrm{e}^{-\mathrm{i}k_2x}+C_0R_6\mathrm{e}^{-\mathrm{i}k_3x},\\
\hat{\psi}_0 &= A_0R_1\mathrm{e}^{-\mathrm{i}k_1x}+B_0R_2\mathrm{e}^{-\mathrm{i}k_2x}+C_0R_3\mathrm{e}^{-\mathrm{i}k_3x},\\
\hat{\phi}_0 &= A_0\mathrm{e}^{-\mathrm{i}k_1x}+B_0\mathrm{e}^{-\mathrm{i}k_2x}+C_0\mathrm{e}^{-\mathrm{i}k_3x}.
\end{aligned} \tag{44}$$

Constants A_0, B_0 and C_0 can be found from the following nodal conditions:

$$\hat{u}_0(x=0)=\hat{q}_1, \quad \hat{\psi}_0(x=0)=\hat{q}_2, \quad \hat{\phi}_0(x=0)=\hat{q}_3. \tag{45}$$

The forces within the element can be expressed using the formulas from Eq. (35). The nodal forces can be found using the following nodal conditions:

$$\begin{aligned}
\hat{F}_1 &= (2\mu+\lambda)A\frac{\partial\hat{u}_0}{\partial x}+\lambda A\hat{\psi}_0 \quad \text{for } x=0,\\
\hat{F}_2 &= \mu I\left(\frac{\partial\hat{\psi}_0}{\partial x}-24\frac{\hat{\phi}_0}{h}\right) \quad \text{for } x=0,\\
\hat{F}_3 &= \frac{48}{5}(2\mu+\lambda)I\frac{\partial\hat{\phi}_0}{\partial x} \quad \text{for } x=0.
\end{aligned} \tag{46}$$

The square and symmetric dynamic stiffness matrix $\mathbf{K}_{\mathrm{dt}}$ of the throw-off spectral element based on the three-mode theory can be calculated by taking into account the formulas for the axial displacement and the lateral contractions and using the formulas for calculating constants A_0, B_0 and C_0. The aforementioned expressions

allow expressing the nodal forces as a function of the nodal displacements. A detailed form of the dynamic stiffness matrix for the spectral rod throw-off element based on the three-mode theory can be found in Appendix B, Eq. (B.4).

6. Numerical examples

The main idea of these numerical calculations is to demonstrate wave propagation phenomena in a rod for the different theories. The results obtained for the elementary, the Love, the Mindlin–Herrmann and the three-mode theories are presented and discussed below.

Computations were carried out for a cantilever steel rod of the following dimensions: length 4 m, width 0.02 m, height 0.02 m. The following material properties are utilised: Young's modulus 210 GPa, Poisson ratio 0.3 and density 7850 kg/m^3. Two different signals were used as a source of propagating waves. Fig. 2 illustrates the comparison of analysed signal shapes, duration times and their FFTs. Each of the signals presented is a so-called 'package' obtained from the multiplication of a triangle and a sinusoidal function. The signal marked as case (a) is a slower signal assumed to last for 0.3 ms. It allows excitation of waves of frequencies up to 80 kHz. The faster signal presented as case (b) lasts for 0.15 ms and allows excitation of waves of frequencies up to 160 kHz.

The next figure (Fig. 3) illustrates the results obtained for the elementary and the Love rod theories. Absolute wavenumbers obtained from the two theories are first presented as a function of the excitation frequency. It is clear that for the data used, differences between the wavenumbers appear above 95 kHz. For lower frequencies the wavenumbers are virtually the same for the two models considered.

Fig. 4 illustrates the absolute wavenumbers obtained for the Mindlin–Herrmann theory. The wavenumber corresponding to the first mode shows similar behaviour to that for the Love theory. The second mode has a cut-off frequency. This frequency is inversely proportional to the thickness or the radius of the rod which means that it increases for slender rods. For better understanding the real and the imaginary parts of wavenumbers are shown separately in Figs. 5 and 6.

The next two figures present a comparison of reflected signals obtained for the elementary and modified theories. For better illustration of differences the accelerations calculated for all the models are normalized according to their maximum value. Fig. 7 presents a comparison of results obtained for the two excitation signals tested. The first plot (Fig. 7(a)) illustrates the differences in the reflected signal obtained for the elementary and Love theories for the slower signal from Fig. 2(a), the second plot (Fig. 7(b)) shows the

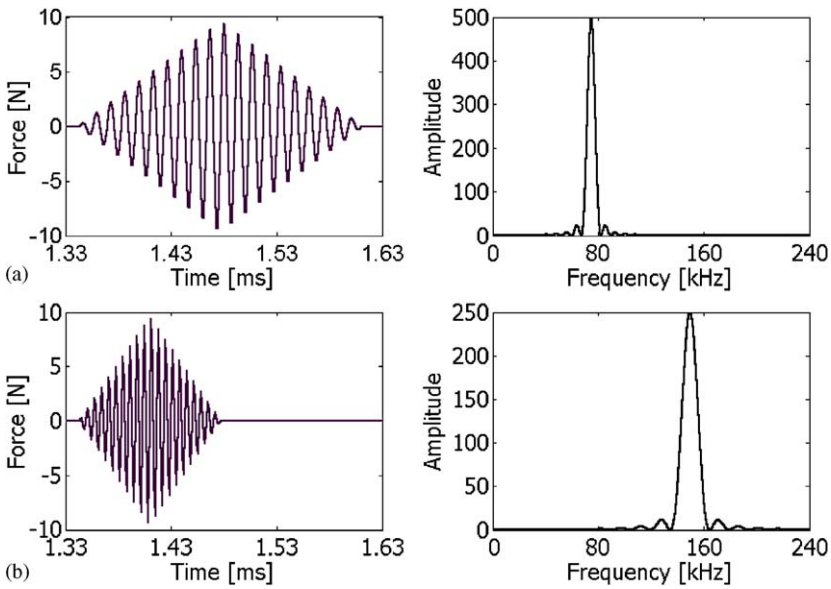

Fig. 2. Comparison of test excitation signals in time and frequency domains.

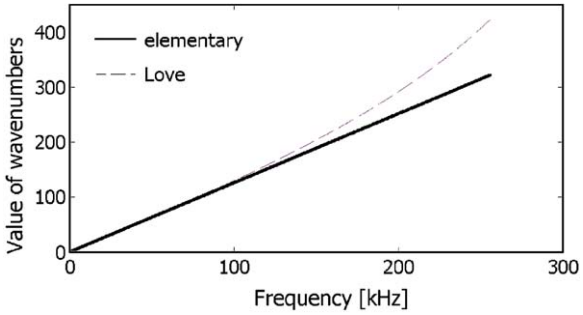

Fig. 3. Absolute values of the wavenumbers obtained from the elementary (___) and Love (– – –) theories.

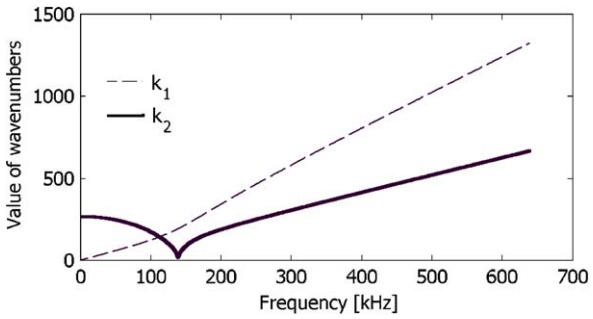

Fig. 4. Absolute values of the wavenumbers obtained from the two-mode theory, (– – –) k_1, (___) k_2.

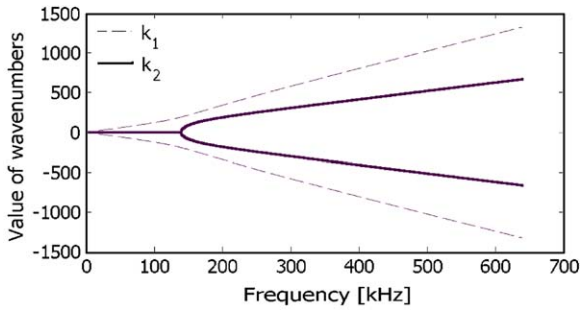

Fig. 5. Real part of the wavenumbers obtained from the two-mode theory, (– – –) k_1, (___) k_2.

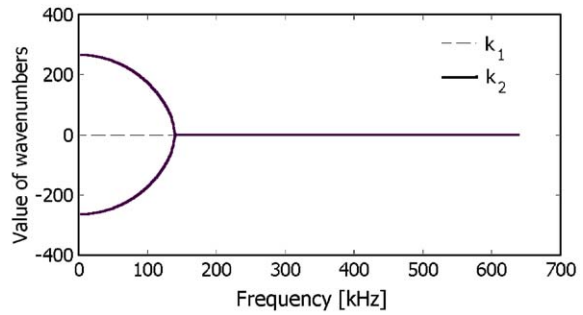

Fig. 6. Imaginary part of the wavenumbers obtained from the two-mode theory, (– – –) k_1, (___) k_2.

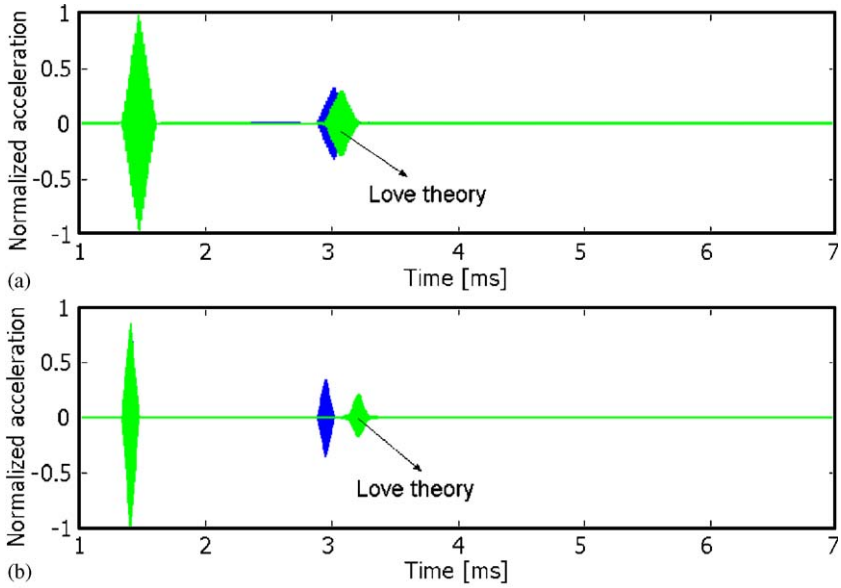

Fig. 7. Reflected signals obtained from the elementary and Love theories: (a) for the slower excitation signal; (b) for the faster excitation signal.

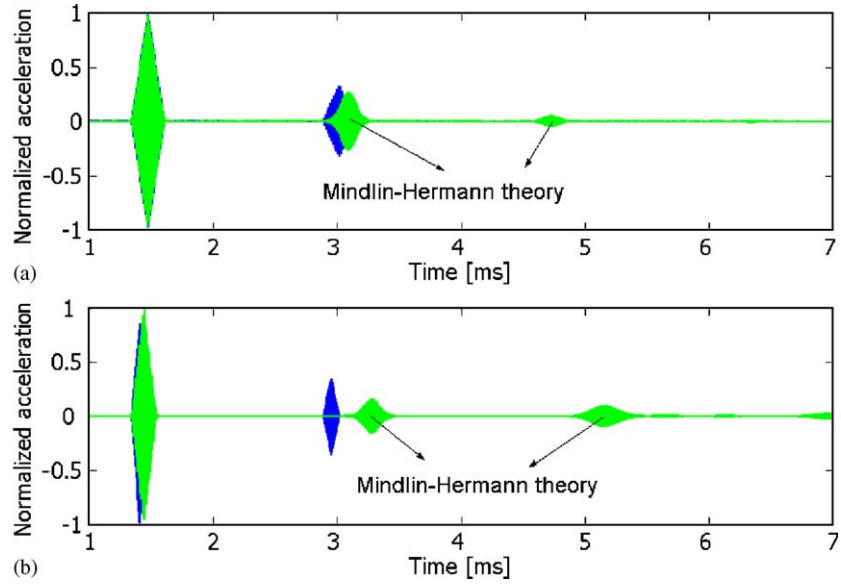

Fig. 8. Reflected signals obtained for the elementary and Mindlin–Herrmann theories: (a) for the slower excitation signal; (b) for the faster excitation signal.

differences for the faster signal shown in Fig. 2(b). It can be seen that more visible differences between the results can be observed for higher frequencies excited by the input signal.

Fig. 8 presents a comparison of results obtained for both excitation signals, for the models based on the elementary and Mindlin–Herrmann rod theories. The meaning of the plots is the same as in Fig. 7. The differences between the results for the models are much more visible when the input signal excites higher frequencies. As can be noticed from Fig. 8(b) some additional reflections appeared with the Mindlin–Herrmann theory, which were not present in the case of the elementary or Love theories.

The contribution of the second wave mode to the vibration is presented in Fig. 9. The plot gives the ratio between the longitudinal mode U and the rotation mode Ψ. As the wavenumbers can be complex three plots showing the contribution to the real, imaginary and the absolute values ((a), (b) and (c), respectively) are presented. It can be concluded that in the frequency range considered (up to 0.14 MHz) the wave amplitude associated with the second mode (Ψ) is purely real. For higher frequency values the wave has imaginary part only which means that the contribution of the second mode (Ψ) to the vibration is decaying. This leads to the conclusion that the Mindlin–Herrmann theory used for higher frequency ranges gives results which have no physical meaning.

The following figures illustrate the frequency dependence of the wavenumbers calculated for three-mode theory. Fig. 10 shows the change in the absolute value of the wavenumbers. The wavenumber for the first mode shows similar behaviour to the first wavenumber for the Love theory. The second and third mode have

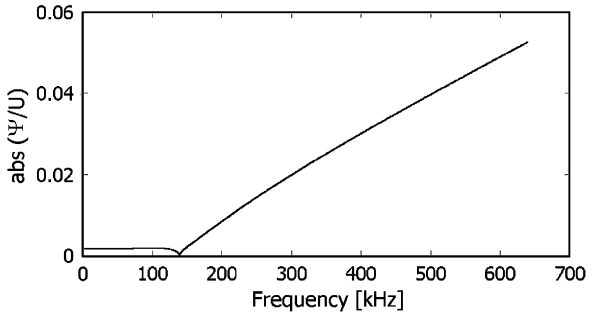

Fig. 9. The contribution of the second wave mode to the vibration.

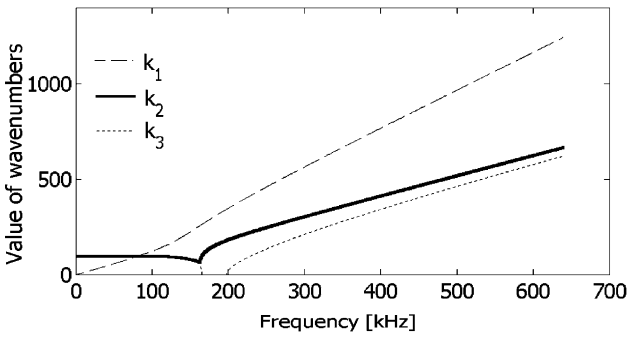

Fig. 10. Absolute values of the wavenumbers obtained from the three-mode theory, (– – –) k_1, (___) k_2, (· · · ·) k_3.

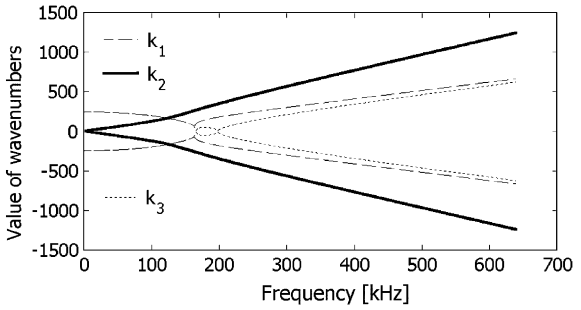

Fig. 11. Real part of the wavenumbers obtained from the three-mode theory, (– – –) k_1, (___) k_2, (....) k_3.

also cut-off frequencies. These frequencies are inversely proportional to the thickness or radius of the rod. Real and imaginary parts of each wavenumber are shown in Figs. 11 and 12.

Next figure presented (Fig. 13) illustrates the differences between the elementary and three-mode theories based on responses recorded for excitation signals from Fig. 2. It can be seen from the graphs that the differences between the results for the two models are considerable; this may be due to the fact that the excitation frequency is higher than the cut-off frequency (Fig. 13(b)). For this high frequency signal the dissipation of the reflected signals for the analysed example is clearly visible. It may also be noticed that as in the case of the Mindlin–Herrmann theory, additional reflection appear for the faster signal for the three-mode theory as well. They were not present in the case of the elementary or Love theories. It is worth mentioning that due to the fact that within this frequency range the third mode is not excited, results obtained for the Mindlin–Hermann and three-mode theories are very similar.

The contribution of the second and third wave mode to the vibration of the rod is presented in Fig. 14. It shows the real, imaginary and the absolute values (marked as (a), (b) and (c) respectively) of the ratio between the longitudinal mode U and the two rotation modes Ψ and Φ. It can be seen that in the frequency range considered, when the real part of the rotation mode share is taken into account for higher frequencies the contribution of the second mode increases, while the contribution of the first rotation mode stays at the same

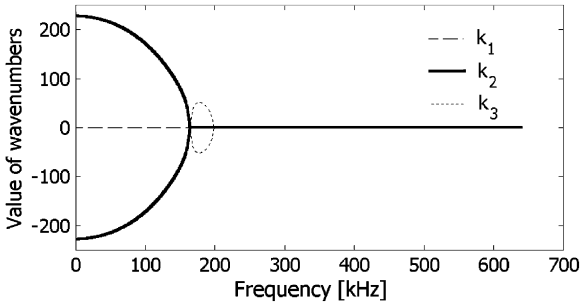

Fig. 12. Imaginary part of the wavenumbers obtained from the three-mode theory, (– – –) k_1, (___) k_2, (· · · ·) k_3.

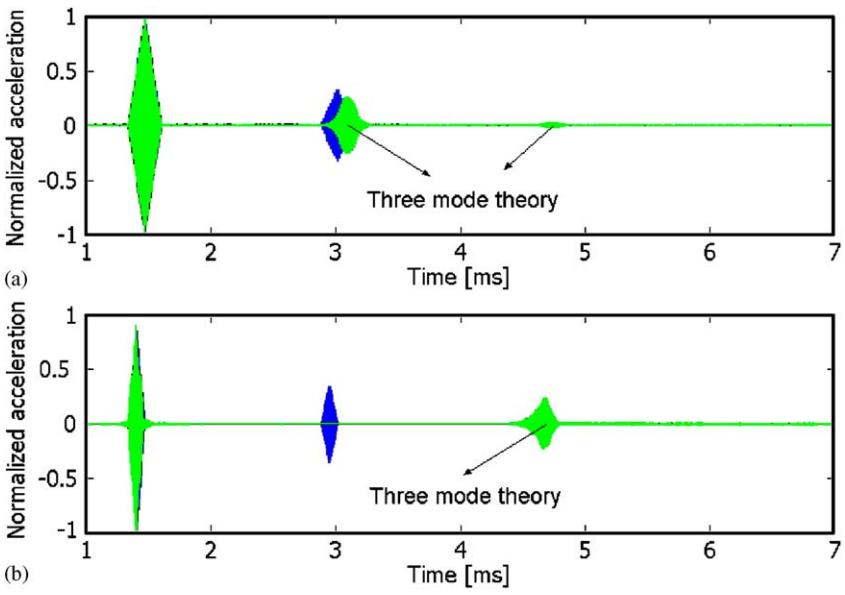

Fig. 13. Reflected signals obtained for the elementary and three-mode theories: (a) for the slower excitation signal; (b) for the faster excitation signal.

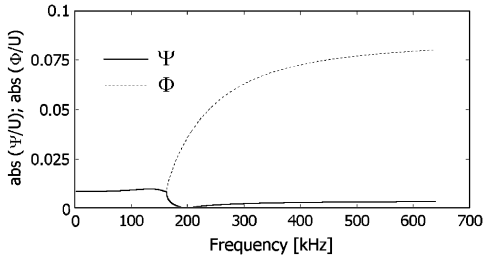

Fig. 14. The contribution of the second (___) and third (– – –) wave mode to the vibration.

level. When the imaginary parts of the rotational mode shares are investigated it is concluded that the vibration of the rod is attenuated by the rotational modes. Generally, it is concluded that in the frequency range considered the absolute wave amplitude associated with the second mode (Ψ) is not higher than 1% of the first mode amplitude (U), while the wave amplitude associated with the third mode (Φ) is not higher than 25% of the first mode amplitude (U). For the three-mode theory when higher frequency values are taken into account the Ψ and Φ modes share stay on the same level, which suggests that the three-mode theory is more adequate for higher frequency ranges.

7. Conclusions

The paper presents a family of spectral elements for wave propagation modelling in rod-like structures. The dynamic stiffness matrices based on the Love, Mindlin–Herrmann and three-mode theories for all considered models are developed. The elementary theory assumes a uniform distribution of the axial displacement along the cross section. The Love theory takes into account the additional kinetic energy. The Mindlin–Herrmann theory assumes that the transverse displacement is not negligible, whereas the most advanced model (three-mode theory) takes into account the non-uniform distribution of the axial displacement and the transverse deformation.

The results of numerical calculations demonstrate considerable differences especially for higher frequencies. The differences found between the models are a function of the excitation frequency. When the excitation frequency increases the differences also increases, because the higher modes, not included in the elementary or Love rod theories, are also excited.

The contribution of the additional modes, analysed within the Mindlin–Herrmann and three-mode theories, on the vibration is also investigated. It may be concluded that the Mindlin–Herrmann theory gives proper results for frequencies up to 250 kHz (Fig. 4) which may imply that this sort of performance could be generalisable for other structural systems. For higher frequencies the contribution of the second mode increases and the results obtained may have no physical meaning. This is why in this system for excitation frequencies higher than 250 kHz the three-mode theory should be applied. For this theory the contribution of the second and third mode becomes stable and does not exceed 8% of the first vibration mode.

A practical remark is that specific material and geometrical data are required before choosing a model for the analysis of wavenumbers. When the excitation signal frequency does not excite higher modes the Love theory gives very good results. Otherwise, for signal frequencies which excite higher modes, the Mindlin–Herrmann or the three-mode theory should be applied.

Acknowledgments

The authors are grateful to the support of the Polish Research Council via KBN Grant no. T07C 007 25 entitled: *"Application of Lamb waves for structural damage detection"*. M. Palacz would also thank the Foundation for Polish Science for being granted the Scholarschip for Young Scientists, for 2003.

Appendix A

Appendix A presents the detailed forms of mathematical formulae describing the dynamic stiffness matrices for the developed spectral element based on the Mindlin–Herrmann rod theory. With the equation presented below the unknown constants A_0, B_0, C_0 and D_0 obtained for the spectral rod element based on the Mindlin–Herrmann theory as a function of displacements, can be expressed as

$$\begin{bmatrix} A_0 \\ B_0 \\ C_0 \\ D_0 \end{bmatrix} = \begin{bmatrix} R_1 & R_2 & -R_1p_1 & -R_2p_2 \\ 1 & 1 & p_1 & p_2 \\ R_1p_1 & R_2p_2 & -R_1 & -R_2 \\ p_1 & p_2 & 1 & 1 \end{bmatrix}^{-1} \begin{bmatrix} \hat{q}_1 \\ \hat{q}_2 \\ \hat{q}_3 \\ \hat{q}_4 \end{bmatrix}, \tag{A.1}$$

with $p_1 = e^{-ik_1L}$, $p_2 = e^{-ik_2L}$. Next matrix equation is given to show the formula relating the spectral forces with the spectral displacements (Mindlin–Herrmann rod theory):

$$\begin{bmatrix} \hat{F}_1 \\ \hat{F}_2 \\ \hat{F}_3 \\ \hat{F}_4 \end{bmatrix} = \begin{bmatrix} -ik_1M_1R_1 + M_2 & -ik_2M_1R_2 + M_2 & (ik_1M_1R_1 + M_2)p_1 & (ik_2M_1R_2 + M_2)p_2 \\ -ik_1M_3 & -ik_2M_3 & -ik_1M_3p_1 & -ik_2M_3p_2 \\ (ik_1M_1R_1 - M_2)p_1 & (ik_2M_1R_2 - M_2)p_2 & -ik_1M_1R_1 - M_2 & -ik_2M_1R_2 - M_2 \\ ik_1M_3p_1 & ik_2M_3p_2 & ik_1M_3 & ik_2M_3 \end{bmatrix} \begin{bmatrix} A_0 \\ B_0 \\ C_0 \\ D_0 \end{bmatrix}, \tag{A.2}$$

with $M_1 = (2\mu + \lambda)A$, $M_2 = \lambda A$, $M_3 = \mu IK_1$. After combining the Eq. (A.2) and Eq. (A.1) one obtains the equation with the dynamic stiffness matrix for the spectral rod element based on the Mindlin–Herrmann theory.

For the spectral throw-off element based on the Mindlin–Herrmann theory the matrix relating the unknown constants with displacement is given by

$$\begin{bmatrix} A_0 \\ B_0 \end{bmatrix} = \begin{bmatrix} R_1 & R_2 \\ 1 & 1 \end{bmatrix}^{-1} \begin{bmatrix} \hat{q}_1 \\ \hat{q}_2 \end{bmatrix}, \tag{A.3}$$

whereas the matrix describing spectral forces as a function of the displacement (after taking into account the Eq. (A.3)) looks as follows:

$$\begin{bmatrix} \hat{F}_1 \\ \hat{F}_2 \end{bmatrix} = \begin{bmatrix} -ik_1M_1R_1 + M_2 & -ik_2M_1R_2 + M_2 \\ -ik_1M_3 & -ik_2M_3 \end{bmatrix} \begin{bmatrix} A_0 \\ B_0 \end{bmatrix}. \tag{A.4}$$

Appendix B

Appendix B shows the detailed form of mathematical formulae describing the dynamic stiffness matrices for the developed spectral element based on the three-mode rod theory. For the spectral rod element based on that theory the matrix relating the spectral displacements and the unknown constants is given by

$$\begin{bmatrix} A_0 \\ B_0 \\ C_0 \\ D_0 \\ E_0 \\ F_0 \end{bmatrix} = \begin{bmatrix} R_4 & R_5 & R_6 & R_4p_1 & R_5p_2 & R_6p_3 \\ R_1 & R_2 & R_3 & -R_1p_1 & -R_2p_2 & -R_3p_3 \\ 1 & 1 & 1 & p_1 & p_2 & p_3 \\ R_4p_1 & R_5p_2 & R_6p_3 & R_4 & R_5 & R_6 \\ R_1p_1 & R_2p_2 & R_3p_3 & -R_1 & -R_2 & -R_3 \\ p_1 & p_2 & p_3 & 1 & 1 & 1 \end{bmatrix}^{-1} \begin{bmatrix} \hat{q}_1 \\ \hat{q}_2 \\ \hat{q}_3 \\ \hat{q}_4 \\ \hat{q}_5 \\ \hat{q}_6 \end{bmatrix}, \tag{B.1}$$

with $p_1 = e^{-ik_1 L}$, $p_2 = e^{-ik_2 L}$, $p_3 = e^{-ik_3 L}$. The equation relating the spectral forces with the spectral displacement, like in previously described mathematical formulae is given by

$$\begin{bmatrix} \hat{F}_1 \\ \hat{F}_2 \\ \hat{F}_3 \\ \hat{F}_4 \\ \hat{F}_5 \\ \hat{F}_6 \end{bmatrix} = \begin{bmatrix} -ik_1 M_1 R_4 + M_2 R_1 & -ik_2 M_1 R_5 + M_2 R_2 & -ik_3 M_1 R_6 + M_2 R_3 & (ik_1 M_1 R_4 - M_2 R_1)p_1 & (ik_2 M_1 R_5 - M_2 R_2)p_2 & (ik_3 M_1 R_6 - M_2 R_3)p_3 \\ -ik_1 M_3 R_1 - M_4 & -ik_2 M_3 R_2 - M_4 & -ik_3 M_3 R_3 - M_4 & (-ik_1 M_3 R_1 - M_4)p_1 & (-ik_2 M_3 R_2 - M_4)p_2 & (-ik_3 M_3 R_3 - M_4)p_3 \\ -ik_1 M_5 & -ik_2 M_5 & -ik_3 M_5 & ik_1 M_5 p_1 & ik_2 M_5 p_2 & ik_3 M_5 p_3 \\ (ik_1 M_1 R_4 - M_2 R_1)p_1 & (ik_2 M_1 R_5 - M_2 R_2)p_2 & (ik_3 M_1 R_6 - M_2 R_3)p_3 & ik_1 M_1 R_4 - M_2 R_1 & ik_2 M_1 R_5 - M_2 R_2 & ik_3 M_1 R_6 - M_2 R_3 \\ (ik_1 M_3 R_1 + M_4)p & (ik_2 M_3 R_2 + M_4)p_2 & (ik_3 M_3 R_3 + M_4)p_3 & ik_1 M_3 R_1 + M_4 & ik_2 M_3 R_2 + M_4 & ik_3 M_3 R_3 + M_4 \\ ik_1 M_5 p_1 & ik_2 M_5 p_2 & ik_3 M_5 p_3 & -ik_1 M_5 & -ik_2 M_5 & -ik_3 M_5 \end{bmatrix} \times \begin{bmatrix} A_0 \\ B_0 \\ C_0 \\ D_0 \\ E_0 \\ F \end{bmatrix}, \tag{B.2}$$

where $M_1 = (2\mu + \lambda)A$, $M_2 = \lambda A$, $M_3 = \mu A$, $M_4 = (24/h)\mu I$, $M_5 = \frac{48}{5}(2\mu + \lambda)I$.

In the case of the throw-off spectral element based on the three-mode theory the matrix relating the unknown constants with the spectral displacements is given by

$$\begin{bmatrix} A_0 \\ B_0 \\ C_0 \end{bmatrix} = \begin{bmatrix} R_4 & R_5 & R_6 \\ R_1 & R_2 & R_3 \\ 1 & 1 & 1 \end{bmatrix}^{-1} \begin{bmatrix} \hat{q}_1 \\ \hat{q}_2 \\ \hat{q}_3 \end{bmatrix}. \tag{B.3}$$

The dynamic stiffness matrix is formulated by joining the matrix from Eq. (B.3) with the expressions describing the spectral forces which leads to the following equation:

$$\begin{bmatrix} \hat{F}_1 \\ \hat{F}_2 \\ \hat{F}_3 \end{bmatrix} = \begin{bmatrix} -\mathrm{i}k_1 M_1 R_4 + M_2 R_1 & -\mathrm{i}k_2 M_1 R_5 + M_2 R_2 & -\mathrm{i}k_3 M_1 R_6 + M_2 R_3 \\ -\mathrm{i}k_1 M_3 R_1 - M_4 & -\mathrm{i}k_2 M_3 R_2 - M_4 & -\mathrm{i}k_3 M_3 R_3 - M_4 \\ -\mathrm{i}k_1 M_5 & -\mathrm{i}k_2 M_5 & -\mathrm{i}k_3 M_5 \end{bmatrix} \begin{bmatrix} A_0 \\ B_0 \\ C_0 \end{bmatrix}. \tag{B.4}$$

References

[1] K.J. Bathe, *Finite Element Procedures in Engineering Analysis*, Prentice-Hall, Englewood Cliffs, 1982.
[2] M. Redwood, *Mechanical Waveguides*, Pergamon Press, New York, 1960.
[3] Y.K. Cheung, *Finite Strip Method in Structural Analysis*, Pergamon Press, New York, 1976.
[4] J.F. Doyle, *Wave Propagation in Structures*, Springer, New York, 1997.
[5] J.F. Doyle, A spectrally formulated finite element for longitudinal wave propagation, *International Journal of Analytical and Experimental Modal Analysis* 3 (1988) 1–5.
[6] M. Palacz, M. Krawczuk, Analysis of longitudinal wave propagation in a cracked rod by the spectral element method, *Computers and Structures* 80 (2002) 1809–1816.
[7] M. Krawczuk, M. Palacz, W. Ostachowicz, The dynamic analysis of a cracked timoshenko beam by the spectral element method, *Journal of Sound and Vibration* 264 (2003) 1139–1153.
[8] J.F. Doyle, T.N. Farris, A spectrally formulated finite element for wave propagation in 3-D frame structures, *International Journal of Analytical and Experimental Modal Analysis* 5 (1990) 223–237.
[9] U. Lee, J. Lee, Spectral element method for levy type plates subject to dynamic loads, *Journal of Engineering Mechanics* 25 (1999) 243–247.
[10] J. Kim, J. Cho, U. Lee, S. Park, Modal spectral element for formulation for axially moving plates subjected to in-plane axial tension, *Computers and Structures* 81 (2003) 2011–2020.
[11] M. Krawczuk, M. Palacz, W. Ostachowicz, Spectral plate element for crack detection with the use of propagating waves, *Modern Practice in Stress and Vibration Analysis Trans Tech Publications, Materials Sciences Forum* 440–441, 2003, pp. 187–194.
[12] S.A. Rizzi, J.F. Doyle, A spectral element approach to wave motion in layered solids, *Journal of Vibration and Acoustics* 114 (1992) 569–577.
[13] I.G. Main, *Vibrations and Waves in Physics*, Cambridge University Press, Cambridge, 1993.
[14] R.D. Mindlin, G. Herrmann, A one dimensional theory of compressional wave in an elastic rod, *Proceedings of First US National Congress of Applied Mechanics*, Anaheim, 1950, pp. 187–191.
[15] I.A. Viktorow, *Rayleigh and Lamb Waves in Physical Theory and Applications*, Plenum Press, New York, 1967.